Cancer Cell
Article

Tetraspanin CD37 Directly Mediates Transduction of Survival and Apoptotic Signals

Rosa Lapalombella,[1] Yuh-Ying Yeh,[1] Liwen Wang,[2] Asha Ramanunni,[1] Sarwish Rafiq,[1,3] Shruti Jha,[1] Justin Staubli,[1,3] David M. Lucas,[1,5] Rajeswaran Mani,[1,4] Sarah E.M. Herman,[1,3] Amy J. Johnson,[1,5] Arletta Lozanski,[1] Leslie Andritsos,[1] Jeffrey Jones,[1] Joseph M. Flynn,[1] Brian Lannutti,[10] Peter Thompson,[11] Paul Algate,[12] Scott Stromatt,[12] David Jarjoura,[6] Xiaokui Mo,[6] Dasheng Wang,[5] Ching-Shih Chen,[1,5] Gerard Lozanski,[7] Nyla A. Heerema,[7] Susheela Tridandapani,[8] Michael A. Freitas,[9,13] Natarajan Muthusamy,[1,4,9,13,*] and John C. Byrd[1,4,5,13,*]
[1]Division of Hematology, Department of Internal Medicine
[2]Department of Chemistry
[3]The Integrated Biomedical Research Graduate Program
[4]Department of Veterinary Biosciences
[5]Division of Medicinal Chemistry and Pharmacognosy, College of Pharmacy
[6]Center for Biostatistics
[7]Department of Pathology
[8]Division of Pulmonary Medicine, Department of Internal Medicine
[9]Department of Molecular Virology, Immunology and Medical Genetics
The Ohio State University, Columbus, OH 43210, USA
[10]Gilead Pharmaceuticals Inc, Seattle, WA 98102, USA
[11]OrbiMed Advisors, LLC, New York, NY 10017, USA
[12]Emergent BioSolutions, Seattle, WA 98121-3460, USA
[13]These authors contributed equally to this work
*Correspondence: raj.muthusamy@osumc.edu (N.M.), john.byrd@osumc.edu (J.C.B.)
DOI 10.1016/j.ccr.2012.03.040

SUMMARY

Tetraspanins are commonly believed to act only as "molecular facilitators," with no direct role in signal transduction. We herein demonstrate that upon ligation, CD37, a tetraspanin molecule expressed on mature normal and transformed B cells, becomes tyrosine phosphorylated, associates with proximal signaling molecules, and initiates a cascade of events leading to apoptosis. Moreover, we have identified two tyrosine residues with opposing regulatory functions: one lies in the N-terminal domain of CD37 in a predicted "ITIM-like" motif and mediates SHP1-dependent death, whereas the second lies in a predicted "ITAM motif" in the C-terminal domain of CD37 and counteracts death signals by mediating phosphatidylinositol 3-kinase-dependent survival.

INTRODUCTION

It is generally assumed that tetraspanins are not directly involved in signal transduction, because of the lack of embedded signaling motifs, and that they instead serve as "molecular facilitators" of signal transduction (Maecker et al., 1997). For instance, tetraspanins such as CD53 and CD63 associate with a protein tyrosine phosphatase in rat lymph node cells and a rat mast cell line, respectively (Carmo and Wright, 1995), whereas CD9-mediated signaling in platelets involves activation of the protein tyrosine kinase $p72^{SYK}$ (Ozaki et al., 1995). Tetraspanins can also associate noncovalently with other immune molecules—for example, CD9 and CD63 with integrins (Berditchevski et al., 1995; Rubinstein et al., 1994), CD81 with CD19/CD21 on B cells (Matsumoto et al., 1993), and with CD4 or CD8 on T cells (Imai and Yoshie, 1993) —suggesting that signaling through tetraspanins, possibly following binding to a yet-unidentified ligand, may regulate the functions of key players in immune recognition.

CD37 is a member of the transmembrane 4 superfamily (TM4SF) of tetraspanin proteins, which have four potential

Significance

The signaling role of CD37 in normal and transformed B cells has not been characterized. Our extensive studies have identified a unique function of CD37 as a death receptor in B cells. We have demonstrated that CD37 is a tetraspanin that can directly mediate dual signal transduction through the C- and N-terminal domain. The finding that two independent regions of CD37 exert completely different functions by concurrently activating cell death and survival pathways opens up opportunities for immunotherapy directed at CD37 cell death-mediated signaling in combination with development of small inhibitory peptides or kinase inhibitors that target the C-terminal activation domain to maximize cell death.

membrane-spanning regions (Horejsí and Vlcek, 1991; Wright and Tomlinson, 1994). CD37 is expressed in developing B cells from pre-B to peripheral mature B cell stages, but not plasma cells. T cells, monocytes, and natural killer (NK) cells express very low levels of CD37 (Schwartz-Albiez et al., 1988), and it is absent on platelets and erythrocytes (van Spriel et al., 2004). CD37 forms protein complexes with CD53, CD81, CD82, and class II glycoprotein on the B cell surface that may represent an ion channel or a transporter (Angelisová et al., 1994). Moreover, CD37 is expressed in B cell endosomes and exosomes, reflecting possible involvement in intracellular trafficking or antigen presentation. Targeted inactivation of CD37 in mice revealed no changes in the development of lymphoid organs, but reduced IgG1 levels and alteration of response to T cell–dependent antigens, indicating a possible role for CD37 in T cell–B cell interaction (Knobeloch et al., 2000). Although the precise function of CD37 and its ligand remains unknown, it has been proposed to have a role in signal transduction pathways that affects cell development, activation, and motility (Wright and Tomlinson, 1994). The direct involvement of CD37 in signaling seems unlikely because of short cytoplasmic tails (8 to ~14 amino acids) that lack canonic signaling motifs.

Given its B cell-selective expression, CD37 represents a candidate therapeutic target for B cell malignancies, such as chronic lymphocytic leukemia (CLL). Several peptides, including anti-CD37 SMIP™ (monospecific protein therapeutic, also referred to as SMIP-016), have been shown to induce rapid and potent in vitro direct tumoricidal activity in lymphoma/leukemia cells (Zhao et al., 2007). TRU-016, a humanized SMIP-016, is currently in a phase 1 clinical trial for relapsed CLL and small lymphocytic lymphoma (SLL) (http://www.clinicaltrials.gov/). Other CD37 targeted antibodies are currently in early clinical development (Hallek et al., 2008; Heider et al., 2011). However, the molecular basis of CD37-mediated cell death is unknown.

RESULTS

Identification of Tyrosine-Phosphorylated Proteins following CD37 Ligation Using Nano-LC-MS/MS

Expression of CD37 on CLL cells is variable, with significantly higher expression on IgVH-mutated versus IgVH-unmutated cells (see Figure S1A available online). Death induced by SMIP-016 is dose and time dependent (Zhao et al., 2007) and correlates with CD37 antigen density (Figure S1B), but not prognostic factors associated with poor outcome in CLL (Figures S1C–S1E). How CD37 ligation induces apoptosis is unknown. Treatment of CLL cells with SMIP-016 induces tyrosine phosphorylation of multiple proteins (Figure 1A), as indicated by immunoblot using anti-phosphotyrosine antibody 4G10 (Zhao et al., 2007). To identify these tyrosine-phosphorylated proteins, we undertook a proteomic approach. CLL cells were treated with SMIP-016 or trastuzumab, which does not bind CLL cells because these cells do not express HER2. Trastuzumab therefore is a good negative control to rule out potential Fcγ receptor-mediated signaling. The lysates were separated by SDS-PAGE following immunoprecipitation with 4G10, and the immunoprecipitated proteins were recovered by in-gel digestion. Following a phosphopeptide enrichment step, peptides were analyzed by LC-MS/MS.

Independent experiments from five patients reproducibly identified several tyrosine-phosphorylated proteins, including protein phosphatase non-receptor-type 6 (PTPN6/SHP1) and the SRC family kinase LYN. SMIP-016-induced tyrosine phosphorylation of SHP1 and LYN was confirmed by immunoprecipitation using 4G10, followed by anti-SHP1 or anti-LYN immunoblot analysis, and vice versa (Figure S1F and data not shown). Tyrosine phosphorylation of SHP1 (Yi et al., 1992) has been implicated in cell growth regulation, and loss of SHP1 in leukemia and other malignancies suggest it to be a tumor suppressor (Wu et al., 2003). We first assessed SHP1, SHP2, and PP2A protein levels in CLL (Figure S1G) and found variable expression of these proteins. To determine whether phosphorylation of SHP1 alters its phosphatase activity, we immunoprecipitated SHP1 from CLL patient cells treated with either trastuzumab or SMIP-016 and assessed its tyrosine phosphatase activity. SHP1 purified from SMIP-016-treated cells exhibited increased enzymatic activity relative to trastuzumab control (Figure 1B). SHP1 downregulation by siRNA resulted in almost complete loss of SMIP-016-induced cytotoxicity compared to nonsense siRNA (Figure 1C), supporting that SHP1 is involved in CD37-mediated cell death, which contrasts with SHP1-independent death induced by CD20 ligation (Kheirallah et al., 2010).

We also identified CD37, SHIP-1, and SYK in the LC-MS/MS analysis. CD37 has three tyrosine residues in its cytoplasmic tail. Detailed sequence analysis shows one of them at the N-terminal (N-t) domain within a predicted weak immune tyrosine-based inhibitory motif (ITIM) and the other two at the C-terminal (C-t) domain, with one located in an YxxL context within a single immune tyrosine-based activation motif (ITAM) (Figure 1D). An ITIM is a conserved sequence of amino acids (S/I/V/LxYxxI/V/L) that is found in the cytoplasmic tails of many inhibitory receptors of the immune system. Interaction of ITIM-bearing receptors with their ligands results in SRC family kinase-mediated tyrosine phosphorylation of the ITIM motif and recruitment of other enzymes, such as SHP1 and SHP2, or SHIP-1, an inositol phosphatase, that decrease the activation of cell signaling molecules. Similarly, the two tyrosine residues contained within the ITAM motif (defined by a consensus sequence: YxxI/Lx(6-12)YxxI/L, where x represents any amino acid) are typically phosphorylated by the SRC family of tyrosine kinases. This results in recruitment of SYK, and initiation of downstream cell activation signals leading to proliferation. The observations that (1) LYN and SHP1 are phosphorylated upon CD37 ligation, (2) SHP1 is directly involved in CD37-mediated cell death, and (3) SHP1 is known to bind to weak ITIM suggested that the ITIM-like motif in CD37 N-t might be functional. We confirmed that, in CLL cells stimulated with SMIP-016, CD37 was tyrosine phosphorylated and associated with both SHP1 and LYN (Figures 1E and 1F). Thus, CD37 engages the negative signaling effectors SHP1 and LYN when tyrosine phosphorylated, consistent with the presence of an ITIM.

SMIP-016-Induced Apoptosis Requires Translocation of CD37 into the Lipid Rafts

Lipid rafts are plasma membrane microdomains enriched in gangliosides (glycosphingolipids) and cholesterol that are involved in many signal transduction processes. For instance,

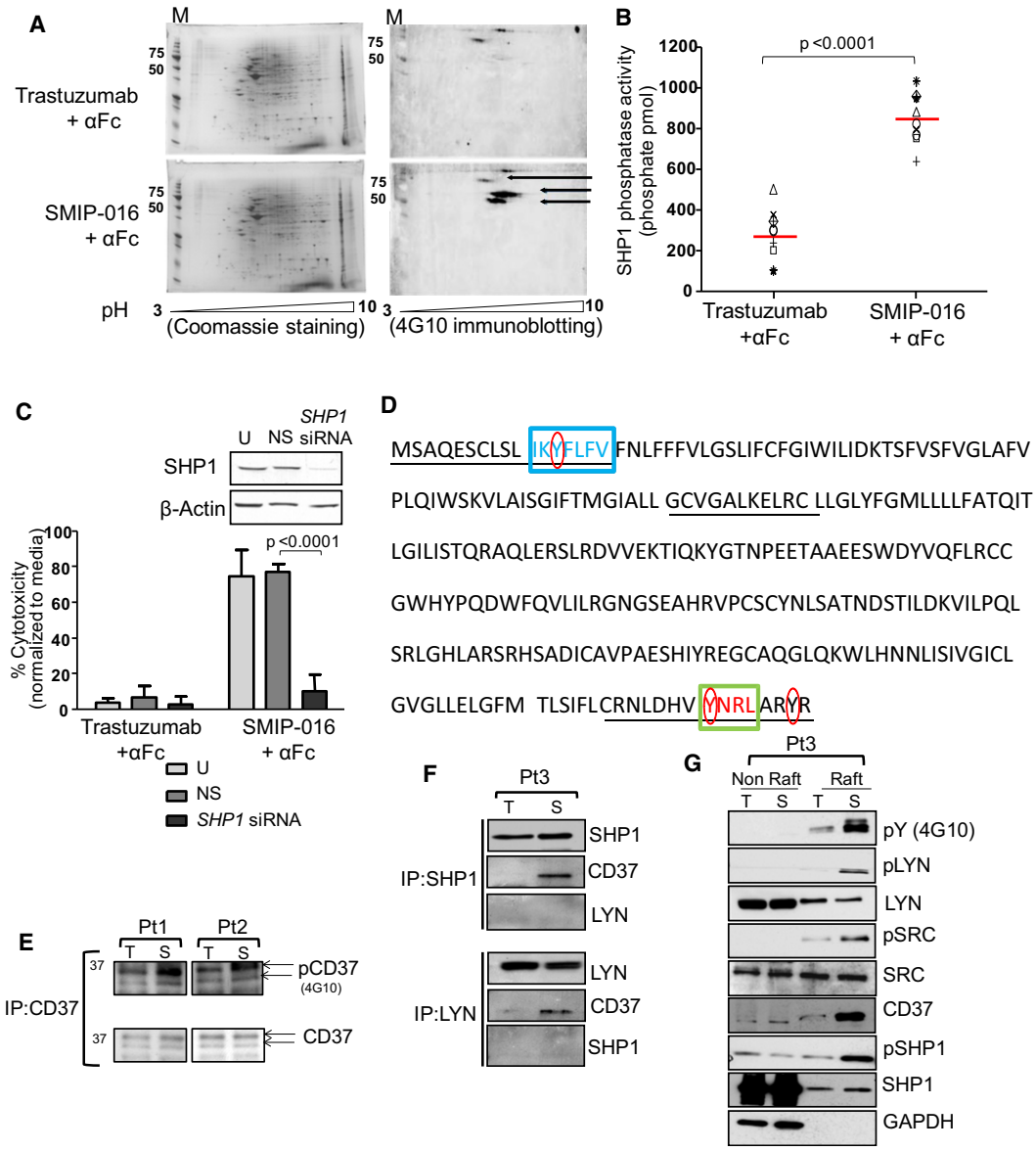

Figure 1. CD37 Ligation Induces Tyrosine Phosphorylation of SHP1, LYN, and CD37

(A) Lysates from trastuzumab+αFc- or SMIP-016+αFc-treated (15 min) CLL cells were analyzed by 2-D electrophoresis. A representative experiment is shown. M, molecular weight marker.

(B and C) SHP1 phosphatase activity of trastuzumab+αFc- or SMIP-016+αFc-treated cells (15 min) (B). Each symbol represents a different CLL patient sample, and red line represents the average (C) SMIP-016-induced cytotoxicity (24 hr) of untransfected CLL cells (U) or CLL cells transfected with *SHP1 siRNA* or a nonsense siRNA (NS), as measured by annexin-V/PI staining (mean ± SD, n = 6). The immunoblot shows protein knockdown by siRNA in a representative sample.

(D) Amino acid sequence of human CD37 protein. Underscored text, intracellular regions; blue box, ITIM-like motif; green box, ITAM motif; red circles, cytosolic tyrosine residues.

(E) Lysates from trastuzumab+αFc-treated (T) or SMIP-016+αFc-treated (S) CLL cells (15 min) were immunoprecipitated with anti-CD37 followed by CD37 or 4G10 immunoblot. Two representative samples out of a total of three are shown.

(F) Lysates from trastuzumab+αFc-treated (T) or SMIP-016+αFc-treated (S) CLL cells (15 min) were immunoprecipitated using anti-SHP1 or anti-LYN followed by SHP1, LYN, or CD37 immunoblot. Representative of four patient samples is shown.

(G) Distributions of CD37, pLYN pSHP1, and pSRC in the non-raft (NR) and lipid raft (R) fractions prepared from CLL cells treated with trastuzumab+αFc (T) or SMIP-016+αFc (S) (15 min). A representative experiment is shown.

See also Figure S1.

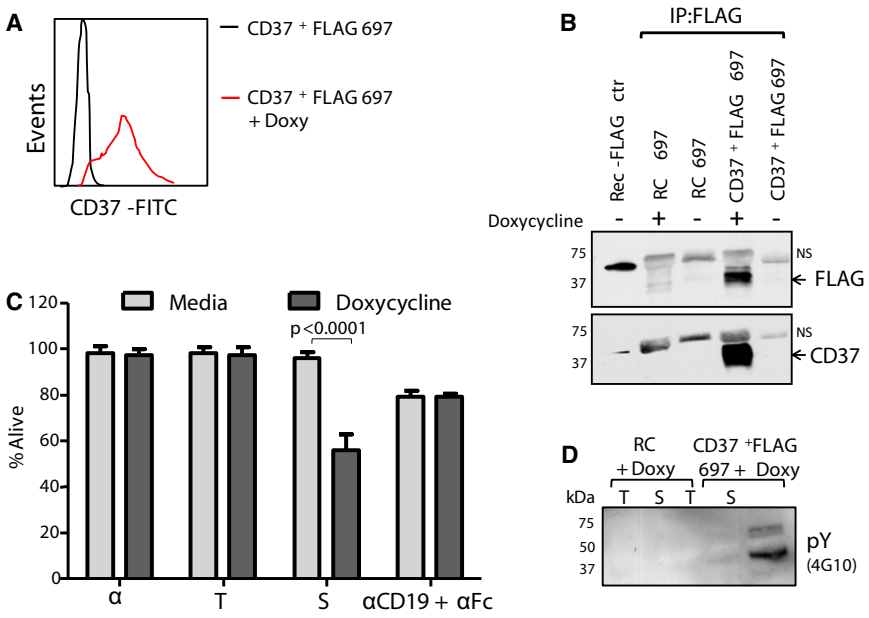

Figure 2. Generation of CD37⁺FLAG 697 Cell Line

(A and B) Expression of CD37 in CD37⁺FLAG 697 cells measured by flow cytometry (A) and immunoblot (B) with or without doxycycline (Doxy) stimulation (24 hr); 697 cells expressing a reverse complement sequence (RC) of CD37 were used as a negative control. NS, nonspecific bands.

(C) CD37⁺FLAG 697 cells were treated for 24 hr with αFc, trastuzumab+αFc (T), SMIP-016+αFc (S), or anti-CD19+αFc, and cytotoxicity was measured by annexin-V/PI (mean ± SD, n = 8).

(D) Lysates derived from trastuzumab+αFc-treated (T) or SMIP-016+αFc-treated (S) CD37⁺ FLAG 697 cells (15 min) were analyzed by immunoblot using 4G10 antibody. Representative of three experiments is shown.

apoptosis induced by rituximab (anti-CD20) requires translocation of CD20 into lipid rafts where it interacts and activates protein tyrosine kinases LYN, FYN, and LCK (Janas et al., 2005; Semac et al., 2003). Upon cross-ligation with SMIP-016, but not trastuzumab, CD37 became associated within membrane lipid rafts along with pSHP1, pLYN, and pSRC (Figure 1G). GAPDH serves as a negative control for the isolation of detergent insoluble membranes, whereas total LYN, SHP1, and SRC serve as a positive control because they have been shown to normally reside in lipid rafts (Mone et al., 2004). The purity of the fractions was confirmed using cholera toxin B subunit-HRP (CT-B) that binds to GM-1, a specific marker of membrane lipid raft (Figure S1I). Cytochalasins inhibit F-actin polymerization, interfere with lipid raft aggregation, and inhibit anti-HLA-DR and anti-CD47 antibody-induced lymphocyte cell death (Truman et al., 1994). Similarly, cytochalasin D (CytD) or latrunculin B (LatB) pretreatment of CLL cells reduced SMIP-016-induced cell death (Figure S1J) and aggregation (Figure S1K).

Generation of CD37⁺FLAG 697 pTet-on Cell Lines

To study in more detail the biology of CD37, we created an inducible CD37⁺FLAG 697 cell line, a derivative of the CD37-negative 697 human acute lymphoblastic leukemia (ALL) cell line, that expresses CD37 upon induction with doxycycline (Figures 2A and 2B). Consistent with the signaling competence of the transfected CD37, treatment of CD37⁺FLAG 697 cells with SMIP-016 significantly induced cytotoxicity (Figure 2C) as well as tyrosine phosphorylation of multiple proteins (Figure 2D). Anti-CD19 was used as a control, because CD19 levels are not affected by doxycycline treatment.

CD37 Is Tyrosine Phosphorylated upon Ligation by SMIP-016

To study phosphorylation events, protein lysates from SMIP-016-treated CD37⁺FLAG 697 cells were immunoprecipitated with 4G10 followed by immunoblot analysis using antibodies specific to proximal signaling targets. These studies identified tyrosine phosphorylation of CD37 (as detected with anti-FLAG), LYN, SHP1, and SYK, following SMIP-016 treatment (Figure 3A). Next, 4G10 immunoprecipitates from SMIP-016-treated CD37⁺ FLAG 697 cells were separated by SDS-PAGE and were subjected to in-gel trypsin digestion followed by a phosphopeptide enrichment step. Proteomics analysis was then performed by neutral loss tandem mass spectrometry on a Thermo Scientific LTQ Orbitrap XL. Five unique peptides of CD37 isoforms A and B were found in SMIP-016-treated but not trastuzumab-treated samples (Figure 3B), with 30% of the sequence covered including phosphorylation at Tyr^{274} (C-terminal region). No alternative proteins were identified from the 37 kDa region of the gel. The presence of CD37 in these immunoprecipitates was independently verified by anti-FLAG immunoblot (data not shown). Furthermore, lysates from SMIP-016 or trastuzumab-treated cells were immunoprecipitated with anti-FLAG antibody and analyzed by 4G10 immunoblot showing the presence of a band of approximately 37 kDa (Figures 3C and 3D), in the SMIP-016 treated lysates, that was abolished by treatment with λ-protein phosphatase (Figure 3D). Coimmunoprecipitation studies using CD37⁺FLAG 697 cells were conducted to confirm that CD37 associates with LYN, SHP1, and SYK upon ligation with SMIP-016 (Figure 3E) and that LYN and SYK were also phosphorylated (Figure 3F), similar to CLL cells. Initial attempts to downmodulate SHP1 in this cell line model using siRNA were unsuccessful, prompting creation of a 697 cell line with stable expression of CD37 and doxycycline-inducible expression of a short hairpin (sh) RNA for SHP1 (shSHP1). In these cells, downmodulation of SHP1 (by 120 hr) resulted in a reduction of SMIP-016-mediated cell death, consistent with the data in primary CLL cells (Figure 3G).

CD37 Possesses Dual Inhibitory and Activation Signaling Functions

To study the relevance of tyrosine phosphorylation in CD37-mediated killing, 697 cell lines carrying mutations or deletions of tyrosine residues in the cytosolic regions of the CD37 molecule were generated (Figure 4A). The deletion of Tyr^{274} or its

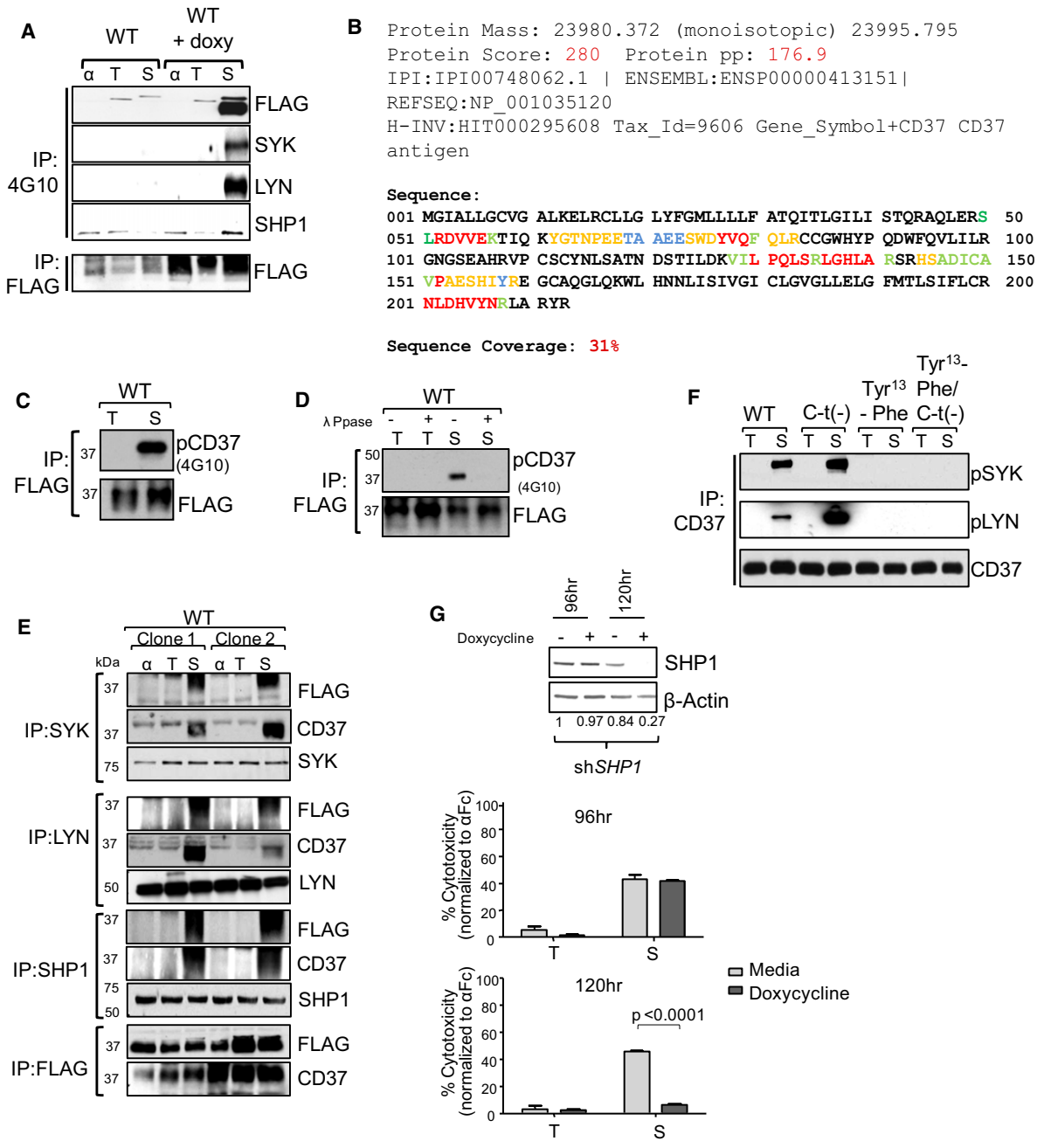

Figure 3. CD37 Is Tyrosine Phosphorylated upon Ligation by SMIP-016

(A) Lysates derived from CD37$^+$FLAG 697 cells (with or without doxycycline) treated with αFc (α), trastuzumab +αFc (T), or SMIP-016+αFc (S) (15 min) were immunoprecipitated with 4G10, followed by immunoblot analysis using antibodies specific to SHP1, SYK, LYN, and CD37. Representative of three experiments is shown. Doxycycline-induced expression of CD37 was verified by anti-FLAG immunoblot (bottom panel).

(B) Sequence coverage of CD37 by phosphoproteomic analysis in SMIP-016-treated CD37$^+$FLAG 697 cells as identified by the MassMatrix software.

(C) Lysates derived from trastuzumab+αFc-treated (T) or SMIP-016+αFc-treated (S) CD37$^+$FLAG 697 cells (15 min) were immunoprecipitated with anti-FLAG, followed by 4G10 immunoblot.

(D) Anti-FLAG-immunoprecipitated lysates from C were treated with λ-protein phosphatase (λ-ppase) followed by 4G10 immunoblot.

(E) Lysates derived from trastuzumab+αFc-treated (T) or SMIP-016+αFc-treated (S) CD37$^+$FLAG 697 cells (15 min) were immunoprecipitated with anti-FLAG, -SHP1, -SYK, or -LYN antibody followed by immunoblot with the indicated antibodies. Results from two different WT cell lines are shown.

(F) Lysates from trastuzumab+αFc-treated (T) or SMIP-016+αFc-treated (S) (15 min) WT, C-t(-), Tyr^{13}-Phe, or Tyr^{13}-Phe/C-t(-) cell lines were immunoprecipitated using anti-CD37, followed by pSYK and pLYN immunoblot.

(G) SMIP-016-induced cytotoxicity of cells with doxycycline-induced downregulation of SHP1 measured by annexin-V/PI staining. Mean ± SD, n = 3. T, trastuzumab+αFc; S, SMIP-016+αFc. The SHP1 protein level is determined using immunoblot. A representative immunoblot is shown.

mutation to phenylalanine (Phe) did not affect surface expression of CD37 but significantly increased the cytotoxic effect of SMIP-016 (Figure 4B). Deletion of the entire C-t cytosolic portion of CD37, which includes Tyr^{274} and Tyr^{280} (Figure 4A), also did not affect surface expression of CD37 but again significantly enhanced the cytotoxic effect of SMIP-016 (Figure 4C) consistent with a regulatory function of this region in CD37-mediated cell death. To test the relevance of Tyr^{13} in the putative N-t ITIM domain, 697 cell lines expressing an N-t truncated CD37 [N-t(-)], a single deletion mutant [Tyr^{13}(-)], or a Tyr^{13}-Phe mutant were generated (Figure 4A). In the N-t(-) and Tyr^{13}(-) cells, no surface CD37 was observed, although CD37 mRNA was still produced and translated (data not shown).The lack of surface expression of CD37 therefore could be attributed to the presence of a membrane localization signal in the deleted portions of the molecule. In contrast, the substitution of Tyr^{13} to Phe did not affect surface expression of CD37 but significantly reduced the cytotoxic effect of SMIP-016 (Figure 4D), indicating that this region positively regulates CD37-mediated cell death, consistent with an ITIM function for this domain. A similar death pattern among the cell lines was also observed for NK cell-mediated antibody-dependent cellular cytotoxicity (ADCC) (Figure S2A), further demonstrating the physiologic relevance of CD37 phosphorylation at the ITIM and ITAM sites.

The effects of N-t and C-t tyrosine deletions on protein-protein interactions and tyrosine phosphorylation were also studied. SMIP-016 treatment of cells induced phosphorylation of both the C-t-deleted and the wild-type (WT) CD37 (Figure 4E) that was sensitive to λ-protein phosphatase treatment (Figure 4F), but the amount of phosphorylation was visibly higher for the C-t-deleted CD37, suggesting that the C-t domain interferes with phosphorylation of the N-t. Furthermore, the lack of the C-t region did not prevent CD37 association with SHP1, LYN, and SYK (Figure 4G) or coassociation of LYN and SHP1 (Figure S2B). In contrast, the replacement of Tyr^{13} with Phe notably reduced SMIP-016-induced CD37 phosphorylation (Figure 4H) and prevented association of SHP1 and LYN with CD37 (Figure 4I) as well as each other (Figure S2B). Together, these data suggest that Tyr^{13} acts in the context of an ITIM motif, phosphorylation of which mediates apoptosis through recruitment and activation of LYN and SHP1. Importantly, the Tyr^{13}-Phe/C-t(-) double mutant CD37 was not phosphorylated when cells were treated with SMIP-016 (Figure 4H). Furthermore, consistent with our previous report (Zhao et al., 2007), herbimycin treatment of the WT and the C-t(-) cell lines prevented cell death (data not shown) and SHP1-CD37 association in both cell lines (Figure 4J). To further demonstrate the phosphorylation and ITIM function of CD37 at the N-t region, we performed a GST pull-down experiment based on the assumption that SH2 domains of SHP1 can bind only to phosphorylated ITIM domains. Lysates derived from 697 cells expressing various forms of CD37 and treated with trastuzumab or SMIP-016 were incubated with GST-SHP1(SH2)N-t, GST-SHP1(SH2)C-t, or GST-SHIP(SH2) fusion proteins, and protein-protein complexes were then purified using glutathione agarose beads (GSH beads). The results show that both GST-SHP1(SH2)N-t and GST-SHP1(SH2)C-t pulled down the WT and the C-t(-)-deleted CD37, but not the Tyr^{13}-Phe or the Tyr^{13}-Phe/C-t(-) CD37. GST and GST-SHIP(SH2) served as negative controls (Figure S2C). The p85 regulatory and the p110 catalytic subunits of phosphatidylinositol 3-kinase (PI3K) have been shown to bind to phosphorylated tyrosines within the ITAM (YxxL) motif of the FcγRIIa in macrophages (Cooney et al., 2001). However, it is not known whether this association is ITAM-mediated and direct, or indirect via an adaptor molecule. We hypothesized that the C-t portion of CD37 negatively regulates cell death by activating a PI3K-dependent survival signaling. Interestingly, WT but not C-t(-) CD37 recruit p85 and p110δ upon stimulation with SMIP-016, indicating that these proteins bind to the C-t portion of CD37 (Figure 4K), consistent with an ITAM function for this domain. The targets of PI3K family kinases include AKT, which is known to mediate B cell proliferation and survival in response to B cell receptor cross-ligation through phosphorylation and inactivation of its downstream target GSK3β. Upon CD37 ligation with SMIP-016, AKT and GSK3β become phosphorylated in WT but not C-t(-) cell lines (Figure 4L). Moreover, treatment of the WT cell line with the PI3K inhibitor LY294002, using a concentration (10 μM) that inhibits PI3K, resulted in increased SMIP-016-mediated cell death up to the level of the C-t(-) cell line (Figure 4M). A similar effect is also seen in primary CLL cells, where the combination of suboptimal doses of SMIP-016 (0.1 μg/ml) with LY294002 or with the PI3Kδ inhibitor CAL-101 is more cytotoxic than any agent alone (Figures S2D and S2E). Surprisingly, PI3Kγ was also recruited upon CD37 cross-ligation. However, its binding was specific to the N-t portion, because it was found to be associated to CD37 even in the absence of the C-t domain (Figure 4N). A functional interaction between PI3K p85/p55 and SHP1 has been shown in T lymphocytes (Cuevas et al., 1999). This interaction was also associated with a reduction in PI3K-mediated phosphorylation of AKT, suggesting that PI3K signaling can be regulated by SHP1. Together, these results suggest that, upon ligation of CD37, two opposing stimuli act simultaneously on AKT and that the outcome for the cell represents a balance between these two counteracting pathways.

CD37 Ligation Mediates Mitochondrial Membrane Depolarization in CLL Cells

We have previously shown that cross-ligation of CD37 by SMIP-016 induces apoptosis of CLL cells (Zhao et al., 2007) as early as 4 hr (data not shown) and peaked at 18 hr. Apoptosis is induced via two main routes involving either the mitochondria (the intrinsic pathway) or the activation of death receptors (the extrinsic pathway). Both pathways converge to induce the activation of caspases, although in the past years, mitochondrial-mediated caspase-independent forms of apoptosis have been reported (Loeffler et al., 2001). We therefore measured mitochondrial membrane depolarization (MMD) of CLL cells in response to SMIP-016 using JC-1 staining. Although no MMD was observed in trastuzumab-treated samples, (Figures 5A and 5B), CD37 ligation resulted in 50% MMD. BIM is a critical BH3 only domain BCL-2 family member protein responsible for mitochondrial-induced apoptosis. Interestingly, CD37 ligation of CLL cells resulted in consistent upregulation of BIM at both the protein (Figure 5C) and mRNA level (Figure 5D), while the protein level of other pro- and antiapoptotic proteins, such as BAX, BCL2, and MCL1, remained unchanged (Figure 5C and Figure S3).

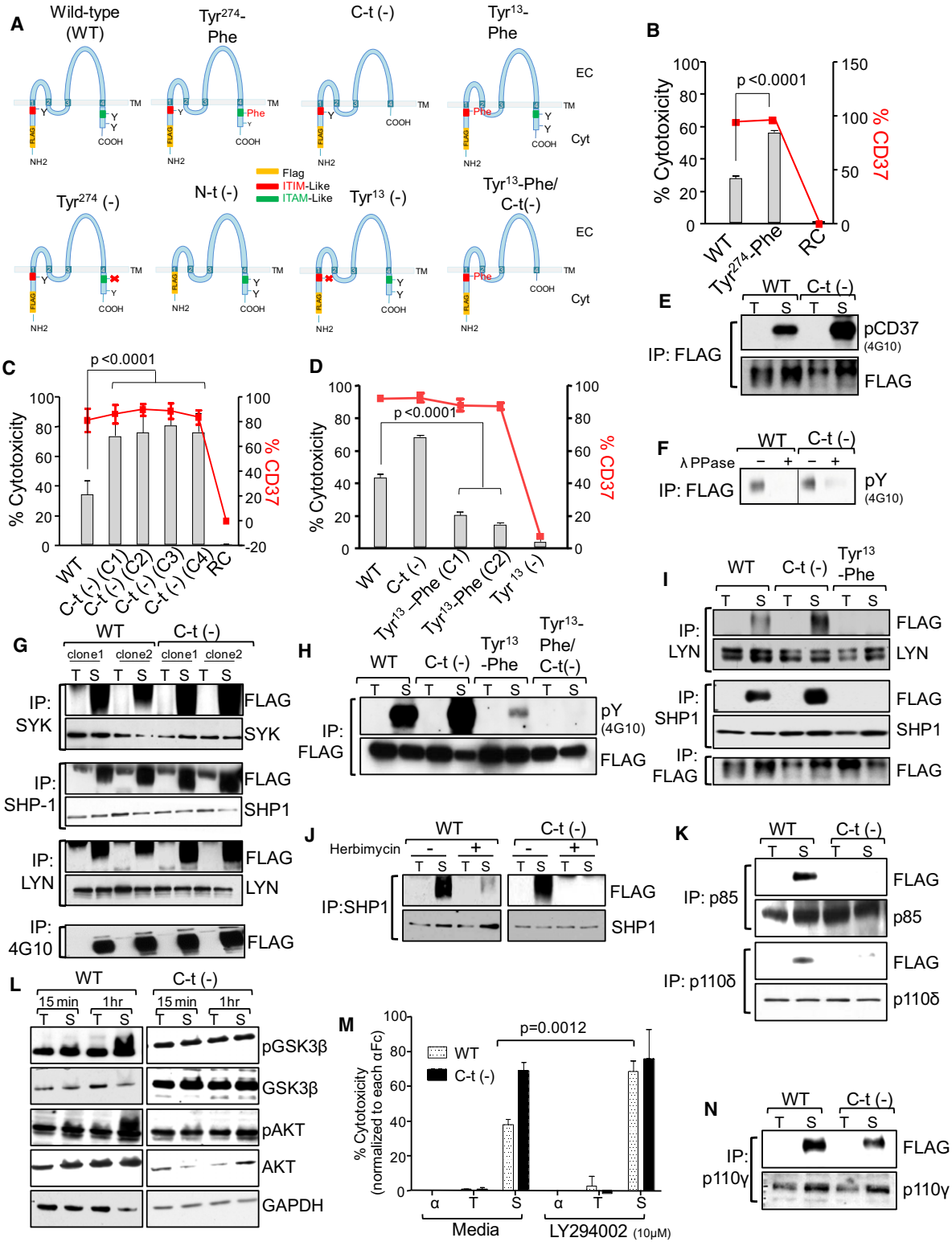

Figure 4. CD37 Possesses Dual Inhibitory and Activation Signaling Function

(A) Schematic representation of the human CD37 protein showing the mutations introduced in the cytosolic regions.

(B–D) CD37^{+}FLAG 697 WT or mutant cell lines were treated with SMIP-016+αFc. Cell death was assessed at 24 hr by annexin-V/PI assay (gray bars). Data shown were normalized to αFc alone (B and C, n = 10; D, n = 16). Expression of CD37 was assessed by flow cytometry (red lines). RC, cells expressing a reverse complement sequence of CD37.

CD37 Cross-Ligation Increases FoxO3a-Dependent Transcription of *BIM*

CLL and a variety of other B cell lymphomas show aberrant expression of TCL1, an oncoprotein with multiple roles in B cell transformation, including active translocation of pAKT to the nucleus (Figure S4A). Cytoplasmic pAKT is modest in nonstimulated CLL cells, whereas nuclear pAKT is dramatically increased (Herman et al., 2010). CD37 ligation by SMIP-016 resulted in a decrease of CD40L-induced PI3K activity (Figure S4B). More importantly, ligation of CD37 in CLL cells decreased basal nuclear pAKT (Figure 6A) and CD40L-induced cytosolic pAKT (Figure S4C). Given the observation that increased pAKT is present in CLL cell nuclei, we hypothesized that this kinase might be influencing FoxO3a, a downstream targets of pAKT and a major transcription factor regulating the expression of *BIM*. As shown in Figure 6B, cross-ligation of CD37 significantly increases the nuclear FoxO3a level. To determine whether SMIP-016 upregulates BIM transcriptionally, a region of the *BIM* promoter containing the FoxO-binding site (FHRE) was cloned into a luciferase reporter construct (Figure 6C) and was transiently transfected into CLL cells. As shown in Figure 6D, *BIM* promoter activity was significantly induced by SMIP-016 treatment of the transfected cells. Furthermore, electrophoretic mobility shift assay (EMSA) using an oligonucleotide sequence derived from the *BIM* promoter region containing FHRE showed increased protein binding in nuclear extract derived from CLL cells treated with SMIP-016, but not the trastuzumab control (Figure 6E). This binding was specific for WT but not mutant FHRE and was prevented by using an excess of cold WT, but not mutant, oligonucleotide probe (Figure 6F). The physical interaction of FoxO3a with the *BIM* promoter in response to SMIP-016 was further confirmed by oligonucleotide pulldown assay (Figure 6G) showing that SMIP-016 treatment increase the binding of FoxO3a to the oligos containing a WT but not mutant FHRE. Next, ChIP assay showed an increased binding of FoxO3a to the endogenous *BIM* promoter in SMIP-016-treated CLL cells (Figure 6H) but not in cells treated with irrelevant antibody (IgG; data not shown). Thus, the increased transcriptional upregulation of *BIM* via FoxO3a following CD37 ligation by SMIP-016 correlates with the increased BIM protein expression described above.

BIM Upregulation Contributes to CD37 Ligation-Mediated Apoptosis

BIM mRNA and protein upregulation was concurrent with its translocation to the mitochondria as well as the cleavage of mitochondrial BAX into p21 and p18 fragments (Figure 7A), which was detected in the enriched mitochondrial fractions only but not in the whole cell lysates (Figure 5C), consistent with the observed MMD following CD37 ligation (Figure 5A). Furthermore, BIM down-modulation by siRNA (Figure S5A) resulted in inhibition of mitochondrial depolarization, with increased intact mitochondria (Figure 7B) and partial reduction of SMIP-016-induced cytotoxicity compared to the scrambled siRNA control (Figure 7C). SHP1 has been implicated in negative regulation of neuronal survival by inhibiting phosphorylation of MAPK/ERK and AKT and increasing BIM expression (Marsh et al., 2003). To determine whether proximal SHP1 activation by SMIP-016 directly contributes to BIM upregulation, siRNA to SHP1 was used. As shown in Figure 7D, SHP1-specific siRNA antagonized BIM upregulation in CLL cells. Collectively, these studies suggest a direct role for SHP1 in downregulating the activity of AKT, which, in turn, inhibits FoxO3a nuclear translocation leading to induction of *BIM* (Figure 7E).

SMIP-016, but not trastuzumab, also induced nuclear translocation of FoxO3a (Figure S5B) and upregulation of BIM in WT CD37^{+}FLAG 697 cells (Figure S5C). AKT phosphorylation was absent in the WT cell line at 18 hr (Figure S5D), corresponding to a later time where BIM induction is seen. Moreover, the deletion of Tyr^{13} but not Tyr^{274} prevented SMIP-016-induced upregulation of BIM in CD37^{+}FLAG 697 cells (Figure S5E). Together, these results support our hypothesis that CD37 directly regulates CLL cell survival.

DISCUSSION

Our study focused on elucidating the role of CD37 in the transduction of apoptotic signals in transformed B cells. Analysis of

(E) Lysates from trastuzumab+αFc-treated (T) or SMIP-016+αFc-treated (S) WT or C-t(-) cells (15 min) were immunoprecipitated with anti-FLAG, followed by 4G10 or FLAG immunoblot.
(F) A portion of the immunoprecipitated lysates from E was treated with λ-protein phosphatase (λ-PPase) and analyzed by 4G10 immunoblot. Irrelevant lanes were cropped out the gel.
(G) Lysates derived from WT or C-t(-) cells treated with trastuzumab+αFc (T) or SMIP-016+αFc (S) (15 min) were immunoprecipitated using anti-SYK, -LYN, -SHP1, or 4G10 antibody, followed by immunoblot analysis with the indicated antibodies.
(H) Lysates derived from WT, C-t(-), and Tyr^{13}-Phe cells treated with trastuzumab+αFc (T) or SMIP-016+αFc (S) (15 min) were immunoprecipitated with anti-FLAG antibody, followed by immunoblot analysis using 4G10 or anti-FLAG antibodies.
(I) Lysates derived from WT, C-t(-), and Tyr^{13}-Phe cells treated with trastuzumab+αFc (T) or SMIP-016+αFc (S) (15 min) were immunoprecipitated using anti-LYN, -SHP1, or 4G10 antibody, followed by immunoblot analysis with the indicated antibodies.
(J) WT or C-t(-) cells were pretreated with either DMSO or herbimycin (10 μM) for 45 min before the addition trastuzumab+αFc (T) or SMIP-016+αFc (S) (15 min). Lysates derived from these cells were immunoprecipitated with anti-SHP1 antibody and analyzed by FLAG and SHP1 immunoblot.
(K) Lysates derived from WT and C-t(-) cells treated with trastuzumab+αFc (T) or SMIP-016+αFc (S) (15 min) were immunoprecipitated with anti-p85 or p110δ antibodies followed by immunoblot with the indicated antibodies. Representative of two experiments is shown.
(L) Lysates derived from trastuzumab+αFc-treated (T) or SMIP-016+αFc-treated (S) WT and C-t(-) cells were analyzed by immunoblot using the indicated antibodies.
(M) WT and C-t(-) cells were pretreated with LY294002 for 45 min before the addition of αFc, trastuzumab+αFc (T), or SMIP-016+αFc (S) . Cell death was measured 24 hr after treatment by annexin-V/PI (n = 15).
(N) Lysates derived from trastuzumab+αFc-treated (T) or SMIP-016+αFc-treated (S) WT and C-t(-) cells (15 min) were immunoprecipitated using p110γ antibody followed by FLAG immunoblot (representative of two experiments). Data are represented as mean ± SD for all the relevant panels.
See also Figure S2.

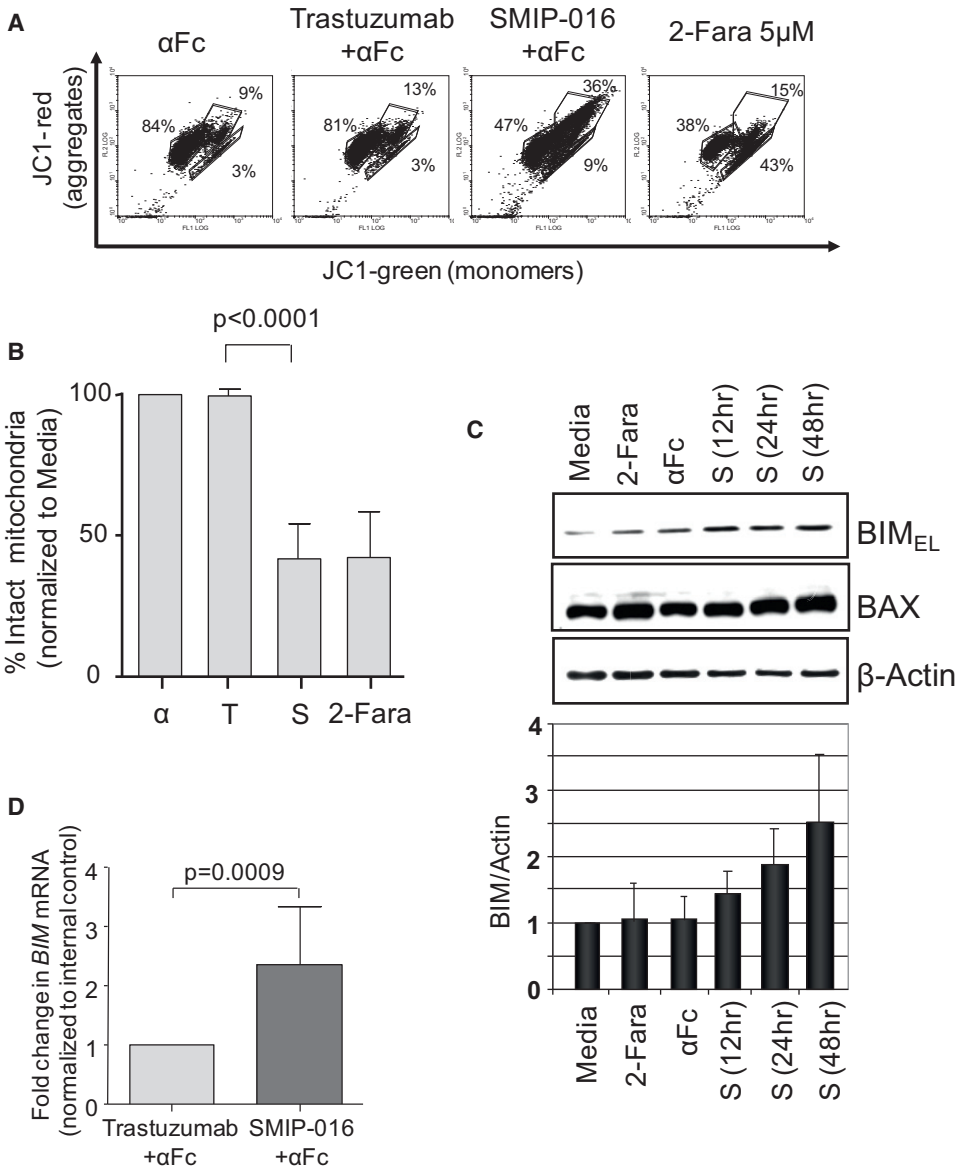

Figure 5. CD37 Ligation Mediates Mitochondrial Membrane Depolarization in Primary CLL Cells

(A and B) Representative data for JC-1 staining of CLL cells treated with αFc, trastuzumab+αFc, SMIP-016+αFc, or 2-fluoro-ara-A (2-Fara) for 12hr (A). A gate was drawn around the population with aggregated JC-1 (intact mitochondria) in untreated cells. Using this gate, the percentage of cells with intact mitochondria in treated samples was then calculated relative to the untreated sample, set at 100% (n = 12) (B).

(C) Lysates derived from CLL cells treated as indicated were analyzed by immunoblot for expression of BIM and BAX. β-Actin was used as loading control. The BIM level relative to the loading control was determined from five immunoblots using different patient samples.

(D) Real-time PCR analysis of *BIM* mRNA in trastuzumab+αFc- or SMIP-016+αFc-treated CLL cells (12 hr, n = 7). Data are represented as mean ± SD for all the relevant panels.

See also Figure S3.

the CD37 protein sequence revealed three tyrosine residues in its cytoplasmic domains with two opposing functions. One of these residues is localized at the N-t domain within the sequence IKYFLFV that resembles an ITIM-motif (V/L/IxYxxV/L) but with an additional residue between the tyrosine and valine. The other two tyrosine residues are located at the C-t domain of CD37, one of which is in a YxxL context within a single ITAM-like signaling motif. ITAM-like motifs were originally described in Dectin-1, and since then, examples of ITAM-based signaling that do not conform precisely to the standard model are becoming increasingly common (Underhill et al., 2005). Moreover, it has been demonstrated that a synthetic peptide based on the phosphorylated single YxxL motif of Dectin-1 binds to SYK (Rogers et al., 2005), suggesting that a single tyrosine phosphorylation might be sufficient to recruit SYK. Through the use of independent biochemical and proteomic approaches, we demonstrate that,

upon cross-ligation, CD37 is tyrosine phosphorylated directly at two distinct tyrosine residues within the N-t (ITIM-like) and C-t (ITAM-like) cytosolic regions. Differences in baseline level of phosphorylation observed in primary CLL cells but not in the $CD37^{+}$FLAG 697 cell line noted in our experiments could be attributed to in vivo stimulation of CLL cells by hitherto unidentified natural ligand for CD37. When a tyrosine in the ITIM is phosphorylated, it forms a docking site for the SRC homology 2 (SH2) recognition domains of the tyrosine phosphatase SHP1. Conversely, ITAM motifs are phosphorylated by SYK. Once phosphorylated the pITAM motif activates SYK, which in turn phosphorylates downstream targets that facilitate survival signaling through PI3K.

We further investigated which complex was recruited by each of these tyrosine domains and demonstrated, as expected, opposing roles for these two tyrosine residues in cell survival. We found that upon ligation of CD37, the N-t tyrosine within the ITIM-like motif becomes phosphorylated and associates with a specific complex of proteins, including LYN, SHP1, SYK, and PI3Kγ, whereas p85 and PI3Kδ were specifically recruited at the C-t domain. Taken together, these data indicate that at least two counteracting signaling pathways originate from ligation of CD37. One pathway acts through phosphorylation and activation of the ITIM-like motif at the N-t of CD37 by LYN kinase, leading to SHP1 recruitment and FoxO3a-dependent *BIM* upregulation and subsequent mitochondrial depolarization and cell death. These ITIM-like and ITAM-like functions also influence NK cell-mediated SMIP cytotoxicity, demonstrating the potential for tumor target antigen signaling influencing innate immune cell killing.

Our data clearly demonstrate that SHP1 is the major driving pathway of death of CD37 ligation but do not exclude the possibility that other signaling pathways, including proximal LYN and SYK, might be involved as well. The second pathway acts through tyrosine phosphorylation of the ITAM-like motif at the CD37 C-t domain, with recruitment and activation of PI3K and AKT, phosphorylation of GSK3β, and promotion of cell survival. The binding of p85 to the phosphorylated YxxL peptide is direct, rather than through a phosphorylated adaptor protein such as SYK. However, these findings do not completely exclude the involvement of an unidentified adaptor protein in p85/PI3K recruitment. This complicated signaling network affords the potential for approaches to augment CD37-directed therapy. Combination treatment with SMIP-016 and the PI3Kδ isoform-specific inhibitor CAL-101 demonstrated synergy, providing clinical rationale for combining these approaches in clinical trials. A diagram of the signaling induced by CD37 ligation is shown in Figure 8.

Although we showed that SMIP-016 efficacy is independent of traditional prognostic factors in CLL, a large variability in cell death was observed, which can be partially attributed to the heterogeneity of CD37 expression in CLL cells and to the simultaneous activation of both pro-death (N-t) and survival (C-t) signaling with SMIP-016 ligation of CD37. No mutations in the CD37 were identified among 120 patients studied (data not shown), although this cannot exclude that CD37 or SHP1 can become mutated or otherwise altered in resistant cells and warrants further study. Additionally, the mechanism by which BIM induction occurs with the CD19 antibody warrants further study.

In summary, we demonstrated herein (1) that CD37 can function as a death receptor in B cells, (2) the presence of two distinct regulatory motifs with opposing functions within the same molecule, and (3) a direct involvement of a tetraspanin in cell death signaling in CLL cells.

EXPERIMENTAL PROCEDURES

Cell Isolation

Blood was obtained from patients with CLL as defined by 2008 IWCLL criteria (Cheson et al., 1996; Hallek et al., 2008). All patients provided informed consent under an Ohio State University Institutional Review Board-approved protocol. CLL B cells were isolated and cultured as previously described (Lapalombella et al., 2010). The purity of tumor cells in the enriched populations was always greater than 95% as detected by dual CD19/CD3 staining.

Chemical Reagents and Cell Treatment

SMIP-016 (5 μg/ml) was produced by Emergent BioSolutions (previously Trubion Pharmaceuticals, Seattle, WA) and is the chimeric parental molecule of TRU-016; 2-fluoro-ara-A (2-Fara, 5 μM), rituximab (10 μg/ml), and trastuzumab (10 μg/ml) were obtained from the OSU pharmacy; goat anti-human IgG (αFc, at 5X antibody concentration) was purchased from Jackson ImmunoResearch Laboratories; sodium stilbogluconate and LY294002 were obtained from Sigma (St. Louis, MO); and FITC-labeled annexin V and propidium iodide (PI) were purchased from BD PharMingen, (San Diego, CA).

Protein Fractionation and Immunoblotting

Cytosolic, nuclear, and mitochondrial fractions were prepared using reagents from Pierce (Rockford, IL) according to the manufacturer's directions. Immunoblots were preformed as described elsewhere (Lapalombella et al., 2010). A detailed list of antibodies used can be found in the Supplemental Information.

Quantitative RT-PCR

cDNA was prepared as previously described (Lapalombella et al., 2008). Primers and probes were obtained from Applied Biosystems (Life Technologies, Carlsbad CA). The expression of *BIM* relative to the internal control gene was calculated by plotting the Ct (cycle number required to reach detection threshold), and the average relative expression for each group was determined using the comparative method (Livak and Schmittgen, 2001). Also see Supplemental Information for additional details.

Chromatin Immunoprecipitation

Chromatin immunoprecipitation assay was performed using the MagnaEZ ChIP Assay Kit (Millipore) according to the manufacturer's standard protocol (Das et al., 2004). DNA was quantified using real-time RT-PCR with SYBR green incorporation (Applied Biosystems). Also see Supplemental Information for additional details.

Immunoprecipitation and Coimmunoprecipitation

Cell lysates were prepared in RIPA (for immunoprecipitation) or Co-IP buffer (for coimmunoprecipitation). A detailed procedure is provided in Supplemental Information.

Electrophoretic Mobility Shift Assays

EMSA procedure and sequence of the ^{32}P-labeled *BIM* promoter probes are described in Supplemental Information.

Oligonucleotide Pull-Down Assay

Oligonucleotide pull-down assays were performed as previously described (Essafi et al., 2005). The detailed procedure is described in Supplemental Information.

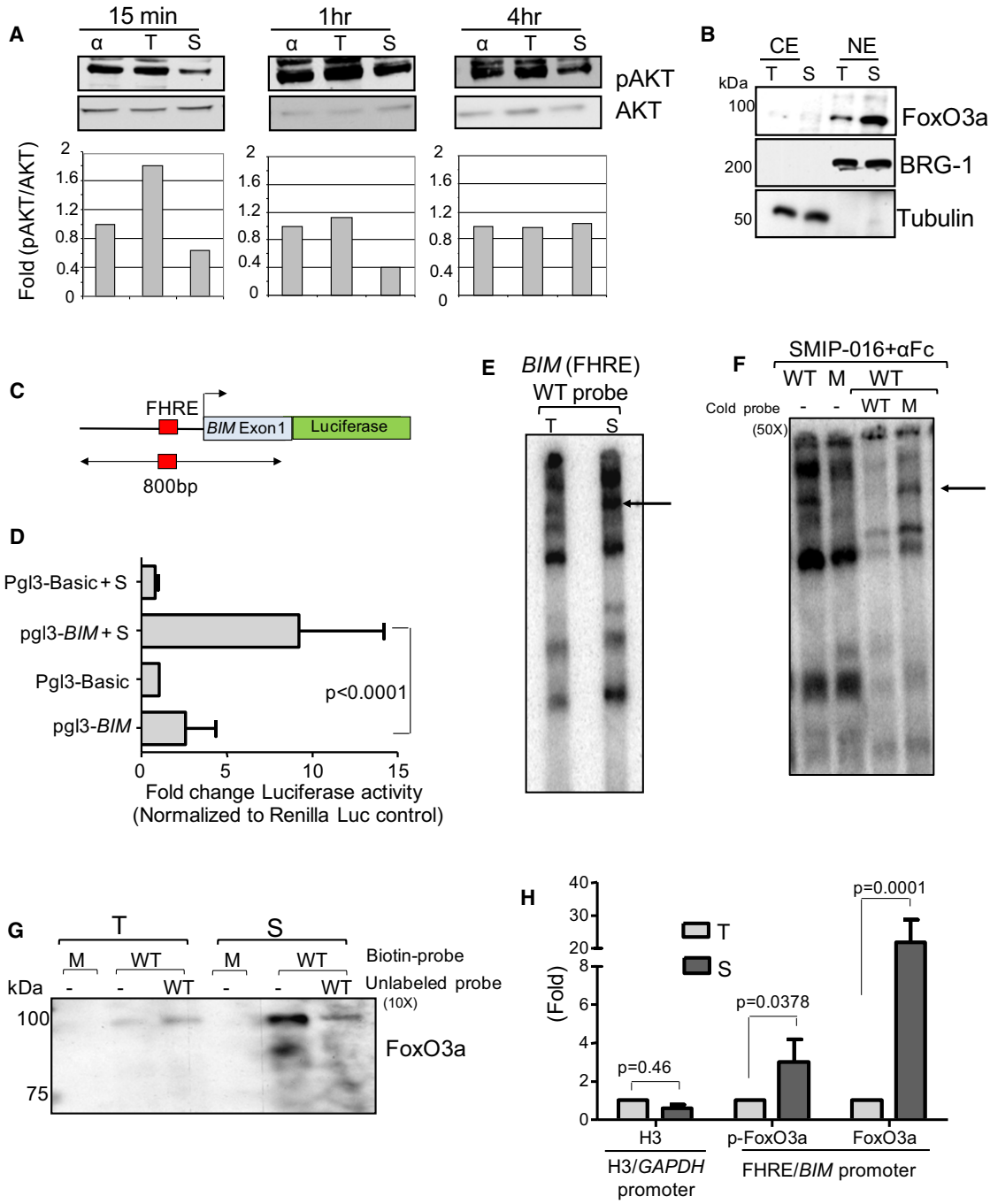

Figure 6. CD37 Cross-Ligation Increases FoxO3a-Dependent Transcription of *BIM*

(A) Top, immunoblot of nuclear extracts derived from αFc, trastuzumab+αFc-treated (T) or SMIP-016+αFc-treated (S) CLL cells; bottom, quantization of the pAKT/total AKT signals in the immunoblots.

(B) Immunoblot analysis of nuclear extracts (NE) and cytoplasmic extracts (CE) from CLL cells stimulated with trastuzumab+αFc (T) or SMIP-016+αFc (S) using FoxO3a antibody. BRG-1 and Tubulin were used to confirm quality of the separations.

(C) Schema of the Pgl3-*BIM* reporter construct that includes the reported FoxO3a binding site (FHRE) in the *BIM* promoter.

(D) Luciferase activity of CLL cells transfected with Pgl3-Basic or Pgl3-*BIM* reporter constructs along with the Renilla luciferase vector and treated without or with SMIP-016+αFc (S) for 12 hr. All values were corrected for cotransfected renilla activity. Data shown are normalized to trastuzumab+αFc-treated cells (n = 4).

(E) Nuclear extract from trastuzumab+αFc-treated (T) or SMIP-016+αFc-treated (S) CLL cells were incubated with ^{32}P-labeled wild-type (WT) *BIM* probe containing FoxO3a binding site and analyzed by EMSA. Representative of nine patient samples is shown.

(F) Nuclear extract from SMIP-016+αFc-treated CLL cells were incubated with ^{32}P-labeled wild-type (WT) or mutant (M) *BIM* probes in the presence or absence of 50× unlabeled wild-type or mutant *BIM* probes.

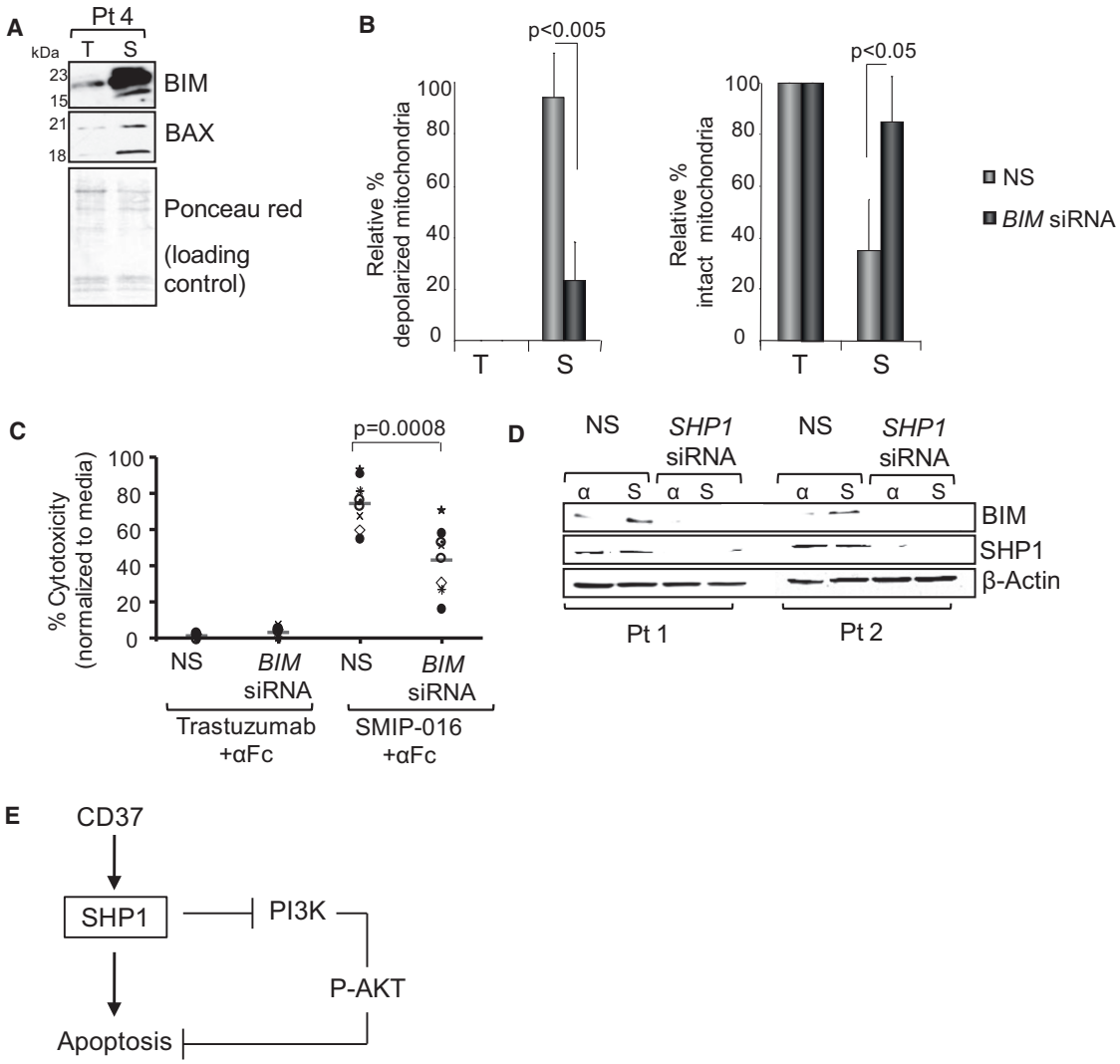

Figure 7. BIM Upregulation Contributes to CD37 Ligation-Mediated Apoptosis

(A) BIM and BAX in mitochondrial extracts from CLL cells treated with trastuzumab+αFc (T) or SMIP-016+αFc (S) for 24 hr were analyzed by immunoblot. Representative of six patient samples is shown.

(B) CLL cells were transiently transfected with *BIM* siRNA for 24 hr and then treated with trastuzumab+αFc (T) or SMIP-016+αFc (S) for an additional 24 hr. Cells were then assayed for mitochondrial membrane integrity by JC-1 staining (mean ± SD; n = 4). NS, nonsense siRNA.

(C) Trastuzumab+αFc or SMIP-016+αFc induced cytotoxicity in CLL cells from (B), as measured by annexin-V/PI staining (24 hr). Each symbol represents a different CLL patient sample; red line represents the average.

(D) BIM and SHP1 immunoblot analysis of CLL cells, from two different patients, transfected with *SHP1*-specific or nonsense (NS) siRNA. Two representative samples out of a total of five are shown.

(E) Diagram depicting CD37-induced apoptosis.

See also Figures S5.

SHP1 Activity Assay

SHP1 phosphatase activity was assessed using the malachite green system (Upstate Biotechnology, Lake Placid, NY) according to the manufacturer's instruction. Detailed protocol is described in Supplemental Information.

PI3K Assay

The PI3K assay was performed on whole-cell lysates from CLL cells. The enzyme-linked immunosorbent assay (Echelon Biosciences, Salt Lake City, UT) was performed according to the manufacturer's instructions as previously described (Herman et al., 2010).

(G) Biotinylated double-stranded oligonucleotides containing FHRE, coupled to streptavidin agarose beads, were incubated with nuclear extracts from trastuzumab+αFc-treated (T) or SMIP-016+αFc-treated (S) CLL cells. Bound proteins were eluted and analyzed by FoxO3a immunoblot. Representative of four patient samples is shown. M, mutant probe; WT, wild-type probe.

(H) Chromatin from trastuzumab+αFc-treated (T) or SMIP-016+αFc-treated (S) CLL cells (12 hr) was analyzed by ChIP assay for binding of FoxO3a to the *BIM* promoter (n = 4). The binding of H3 to the *GAPDH* promoter (H3 element) was also evaluated as a control because SMIP-016 does not affect *GADPH* expression. Data are represented as mean ± SD for all the relevant panels.

See also Figure S4.

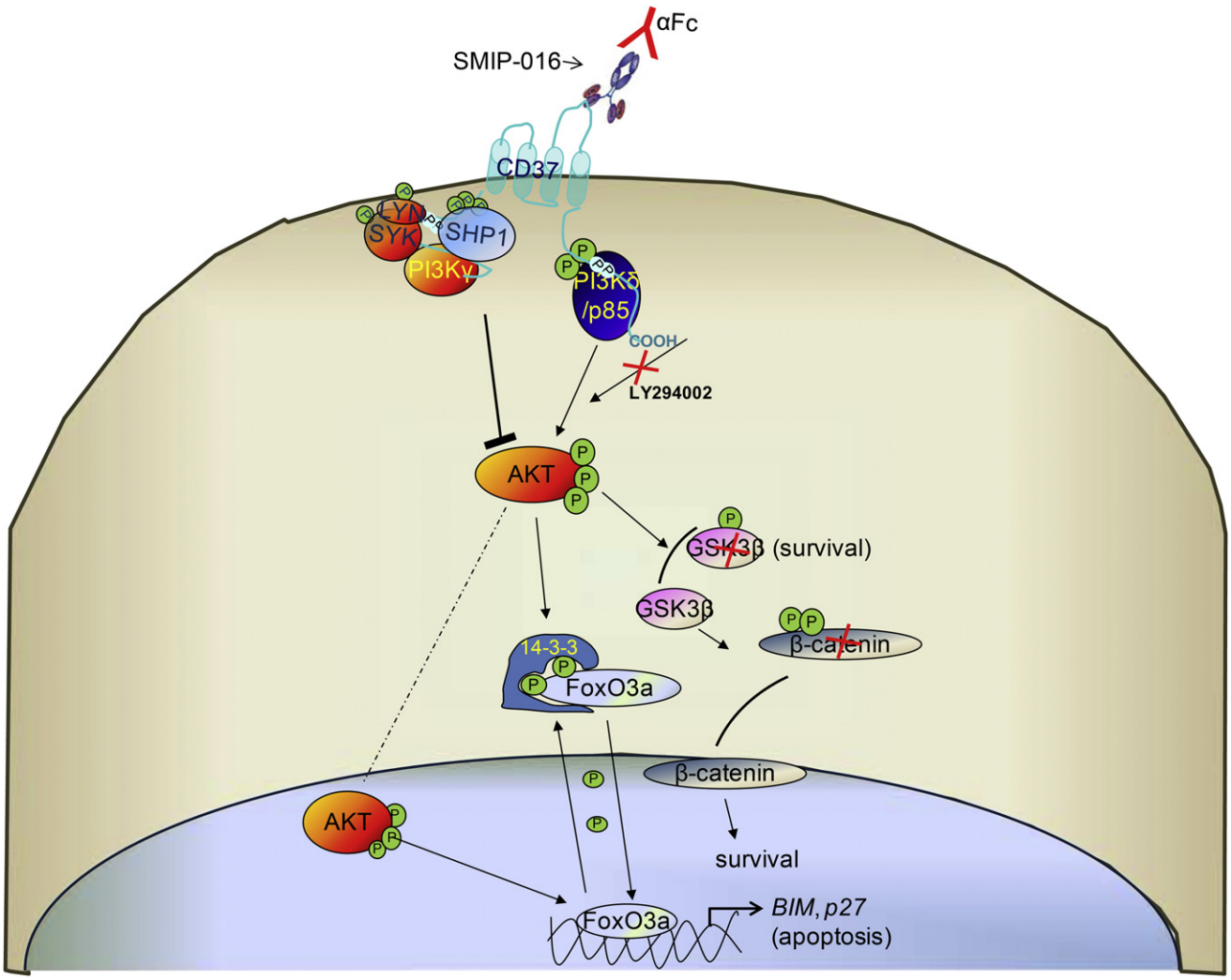

Figure 8. Schema for SMIP-016-Induced Cytotoxicity

Upon ligation of CD37, two signaling pathways are generated, one acting through phosphorylation of the N-t ITIM-like motif of CD37 by LYN kinase, leading to SHP1-dependent *BIM* upregulation and cell death. A second pathway acts through tyrosine phosphorylation of the C-t ITAM-like motif of CD37 with activation of GSK3β and promotion of cell survival.

Apoptosis and Mitochondrial Membrane Depolarization Studies

Cell death was assessed using annexin-V and propidium iodide (PI) flow cytometry-based assays (BD Biosciences, San Diego, CA) as previously described (Lapalombella et al., 2008). Mitochondrial membrane potential changes were assessed using the voltage-sensitive lipophilic cationic dye 5,5′,6,6′-tetrachloro-1,1′,3,3′-tetraethylbenzimidazolyl carbocyanine iodide (JC-1; Molecular Probes, Eugene, OR) as previously described (Alinari et al., 2011).

Transient Transfection and *BIM* Luciferase Activity

Luciferase assay was performed as previously described (Lapalombella et al., 2010). The detailed protocol is described in Supplemental Information.

LC-MS/MS Studies

Briefly, after electrophoresis, gels were fixed, washed, and then stained using Coomassie Brilliant Blue. Gels were then trypsin-digested before the peptides were extracted and concentrated under vacuum to a final volume of 20 μL. Peptides were separated by reversed-phase HPLC and analyzed by mass spectrometry. The detailed procedure is described in the Supplemental Information.

Retrovirus Vectors and Generation of CD37$^+$ Cell Lines

Construction of the human CD37 FLAG in pRetro-tight-puro or pBabe-puro and retroviral infection to establish the CD37$^+$FLAG 697 cell line are described in detail in Supplemental information.

Statistical Analyses

All analyses were performed by the OSU Center for Biostatistics. A detailed description of statistical tests used is included in the Supplemental Information.

SUPPLEMENTAL INFORMATION

Supplemental Information includes five figures and Supplemental Experimental Procedures and can be found with this article online at doi:10.1016/j.ccr.2012.03.040.

ACKNOWLEDGMENTS

We thank the members of the CLL Experimental Therapeutics laboratory, Freitas laboratory, and Dr. Guido Marcucci, for critical comments and review

of the final manuscript, and Dr. Shu-Huei Wang for *BIM* promoter reporter plasmids. We are grateful for research support from The Leukemia and Lymphoma Society and the National Cancer Institute (grants P50 CA140158, PO1 CA95426, PO1 CA81534, 1K12 CA133250, and RO1 CA107106). Mr. and Mrs. Michael Thomas, The Harry Mangurian Foundation, and The D. Warren Brown Foundation also supported this work.

P.A. and S.S. are employees of Emergent BioSolutions and have financial interests in TRU-016 development. B.L. is an employee of Gilead Pharmaceuticals and has financial interest in Cal-101 development. P.T. was a past employee of Trubion Pharmaceuticals with financial interest in development of TRU-016.

Received: July 31, 2011
Revised: December 13, 2011
Accepted: March 5, 2012
Published: May 14, 2012

REFERENCES

Alinari, L., Yu, B., Christian, B.A., Yan, F., Shin, J., Lapalombella, R., Hertlein, E., Lustberg, M.E., Quinion, C., Zhang, X., et al. (2011). Combination anti-CD74 (milatuzumab) and anti-CD20 (rituximab) monoclonal antibody therapy has in vitro and in vivo activity in mantle cell lymphoma. Blood *117*, 4530–4541.

Angelisová, P., Hilgert, I., and Horejsí, V. (1994). Association of four antigens of the tetraspans family (CD37, CD53, TAPA-1, and R2/C33) with MHC class II glycoproteins. Immunogenetics *39*, 249–256.

Berditchevski, F., Bazzoni, G., and Hemler, M.E. (1995). Specific association of CD63 with the VLA-3 and VLA-6 integrins. J. Biol. Chem. *270*, 17784–17790.

Carmo, A.M., and Wright, M.D. (1995). Association of the transmembrane 4 superfamily molecule CD53 with a tyrosine phosphatase activity. Eur. J. Immunol. *25*, 2090–2095.

Cheson, B.D., Bennett, J.M., Grever, M., Kay, N., Keating, M.J., O'Brien, S., and Rai, K.R. (1996). National Cancer Institute-sponsored Working Group guidelines for chronic lymphocytic leukemia: revised guidelines for diagnosis and treatment. Blood *87*, 4990–4997.

Cooney, D.S., Phee, H., Jacob, A., and Coggeshall, K.M. (2001). Signal transduction by human-restricted Fc gamma RIIa involves three distinct cytoplasmic kinase families leading to phagocytosis. J. Immunol. *167*, 844–854.

Cuevas, B., Lu, Y., Watt, S., Kumar, R., Zhang, J., Siminovitch, K.A., and Mills, G.B. (1999). SHP-1 regulates Lck-induced phosphatidylinositol 3-kinase phosphorylation and activity. J. Biol. Chem. *274*, 27583–27589.

Das, P.M., Ramachandran, K., vanWert, J., and Singal, R. (2004). Chromatin immunoprecipitation assay. Biotechniques *37*, 961–969.

Essafi, A., Fernández de Mattos, S., Hassen, Y.A., Soeiro, I., Mufti, G.J., Thomas, N.S., Medema, R.H., and Lam, E.W. (2005). Direct transcriptional regulation of Bim by FoxO3a mediates STI571-induced apoptosis in Bcr-Abl-expressing cells. Oncogene *24*, 2317–2329.

Hallek, M., Cheson, B.D., Catovsky, D., Caligaris-Cappio, F., Dighiero, G., Döhner, H., Hillmen, P., Keating, M.J., Montserrat, E., Rai, K.R., and Kipps, T.J.; International Workshop on Chronic Lymphocytic Leukemia. (2008). Guidelines for the diagnosis and treatment of chronic lymphocytic leukemia: a report from the International Workshop on Chronic Lymphocytic Leukemia updating the National Cancer Institute-Working Group 1996 guidelines. Blood *111*, 5446–5456.

Heider, K.H., Kiefer, K., Zenz, T., Volden, M., Stilgenbauer, S., Ostermann, E., Baum, A., Lamche, H., Küpcü, Z., Jacobi, A., et al. (2011). A novel Fc-engineered monoclonal antibody to CD37 with enhanced ADCC and high proapoptotic activity for treatment of B-cell malignancies. Blood *118*, 4159–4168.

Herman, S.E., Gordon, A.L., Wagner, A.J., Heerema, N.A., Zhao, W., Flynn, J.M., Jones, J., Andritsos, L., Puri, K.D., Lannutti, B.J., et al. (2010). Phosphatidylinositol 3-kinase-δ inhibitor CAL-101 shows promising preclinical activity in chronic lymphocytic leukemia by antagonizing intrinsic and extrinsic cellular survival signals. Blood *116*, 2078–2088.

Horejsí, V., and Vlcek, C. (1991). Novel structurally distinct family of leucocyte surface glycoproteins including CD9, CD37, CD53 and CD63. FEBS Lett. *288*, 1–4.

Imai, T., and Yoshie, O. (1993). C33 antigen and M38 antigen recognized by monoclonal antibodies inhibitory to syncytium formation by human T cell leukemia virus type 1 are both members of the transmembrane 4 superfamily and associate with each other and with CD4 or CD8 in T cells. J. Immunol. *151*, 6470–6481.

Janas, E., Priest, R., Wilde, J.I., White, J.H., and Malhotra, R. (2005). Rituxan (anti-CD20 antibody)-induced translocation of CD20 into lipid rafts is crucial for calcium influx and apoptosis. Clin. Exp. Immunol. *139*, 439–446.

Kheirallah, S., Caron, P., Gross, E., Quillet-Mary, A., Bertrand-Michel, J., Fournié, J.J., Laurent, G., and Bezombes, C. (2010). Rituximab inhibits B-cell receptor signaling. Blood *115*, 985–994.

Knobeloch, K.P., Wright, M.D., Ochsenbein, A.F., Liesenfeld, O., Löhler, J., Zinkernagel, R.M., Horak, I., and Orinska, Z. (2000). Targeted inactivation of the tetraspanin CD37 impairs T-cell-dependent B-cell response under suboptimal costimulatory conditions. Mol. Cell. Biol. *20*, 5363–5369.

Lapalombella, R., Yu, B., Triantafillou, G., Liu, Q., Butchar, J.P., Lozanski, G., Ramanunni, A., Smith, L.L., Blum, W., Andritsos, L., et al. (2008). Lenalidomide down-regulates the CD20 antigen and antagonizes direct and antibody-dependent cellular cytotoxicity of rituximab on primary chronic lymphocytic leukemia cells. Blood *112*, 5180–5189.

Lapalombella, R., Andritsos, L., Liu, Q., May, S.E., Browning, R., Pham, L.V., Blum, K.A., Blum, W., Ramanunni, A., Raymond, C.A., et al. (2010). Lenalidomide treatment promotes CD154 expression on CLL cells and enhances production of antibodies by normal B cells through a PI3-kinase-dependent pathway. Blood *115*, 2619–2629.

Livak, K.J., and Schmittgen, T.D. (2001). Analysis of relative gene expression data using real-time quantitative PCR and the 2(-Delta Delta C(T)) method. Methods *25*, 402–408.

Loeffler, M., Daugas, E., Susin, S.A., Zamzami, N., Metivier, D., Nieminen, A.L., Brothers, G., Penninger, J.M., and Kroemer, G. (2001). Dominant cell death induction by extramitochondrially targeted apoptosis-inducing factor. FASEB J. *15*, 758–767.

Maecker, H.T., Todd, S.C., and Levy, S. (1997). The tetraspanin superfamily: molecular facilitators. FASEB J. *11*, 428–442.

Marsh, H.N., Dubreuil, C.I., Quevedo, C., Lee, A., Majdan, M., Walsh, G.S., Hausdorff, S., Said, F.A., Zoueva, O., Kozlowski, M., et al. (2003). SHP-1 negatively regulates neuronal survival by functioning as a TrkA phosphatase. J. Cell Biol. *163*, 999–1010.

Matsumoto, A.K., Martin, D.R., Carter, R.H., Klickstein, L.B., Ahearn, J.M., and Fearon, D.T. (1993). Functional dissection of the CD21/CD19/TAPA-1/Leu-13 complex of B lymphocytes. J. Exp. Med. *178*, 1407–1417.

Mone, A.P., Huang, P., Pelicano, H., Cheney, C.M., Green, J.M., Tso, J.Y., Johnson, A.J., Jefferson, S., Lin, T.S., and Byrd, J.C. (2004). Hu1D10 induces apoptosis concurrent with activation of the AKT survival pathway in human chronic lymphocytic leukemia cells. Blood *103*, 1846–1854.

Ozaki, Y., Satoh, K., Kuroda, K., Qi, R., Yatomi, Y., Yanagi, S., Sada, K., Yamamura, H., Yanabu, M., Nomura, S., et al. (1995). Anti-CD9 monoclonal antibody activates p72syk in human platelets. J. Biol. Chem. *270*, 15119–15124.

Rogers, N.C., Slack, E.C., Edwards, A.D., Nolte, M.A., Schulz, O., Schweighoffer, E., Williams, D.L., Gordon, S., Tybulewicz, V.L., Brown, G.D., and Reis e Sousa, C. (2005). Syk-dependent cytokine induction by Dectin-1 reveals a novel pattern recognition pathway for C type lectins. Immunity *22*, 507–517.

Rubinstein, E., Le Naour, F., Billard, M., Prenant, M., and Boucheix, C. (1994). CD9 antigen is an accessory subunit of the VLA integrin complexes. Eur. J. Immunol. *24*, 3005–3013.

Schwartz-Albiez, R., Dörken, B., Hofmann, W., and Moldenhauer, G. (1988). The B cell-associated CD37 antigen (gp40-52): structure and subcellular expression of an extensively glycosylated glycoprotein. J. Immunol. *140*, 905–914.

Semac, I., Palomba, C., Kulangara, K., Klages, N., van Echten-Deckert, G., Borisch, B., and Hoessli, D.C. (2003). Anti-CD20 therapeutic antibody rituximab modifies the functional organization of rafts/microdomains of B lymphoma cells. Cancer Res. *63*, 534–540.

Truman, J.P., Ericson, M.L., Choqueux-Séébold, C.J., Charron, D.J., and Mooney, N.A. (1994). Lymphocyte programmed cell death is mediated via HLA class II DR. Int. Immunol. *6*, 887–896.

Underhill, D.M., Rossnagle, E., Lowell, C.A., and Simmons, R.M. (2005). Dectin-1 activates Syk tyrosine kinase in a dynamic subset of macrophages for reactive oxygen production. Blood *106*, 2543–2550.

van Spriel, A.B., Puls, K.L., Sofi, M., Pouniotis, D., Hochrein, H., Orinska, Z., Knobeloch, K.P., Plebanski, M., and Wright, M.D. (2004). A regulatory role for CD37 in T cell proliferation. J. Immunol. *172*, 2953–2961.

Wright, M.D., and Tomlinson, M.G. (1994). The ins and outs of the transmembrane 4 superfamily. Immunol. Today *15*, 588–594.

Wu, C., Sun, M., Liu, L., and Zhou, G.W. (2003). The function of the protein tyrosine phosphatase SHP-1 in cancer. Gene *306*, 1–12.

Yi, T.L., Cleveland, J.L., and Ihle, J.N. (1992). Protein tyrosine phosphatase containing SH2 domains: characterization, preferential expression in hematopoietic cells, and localization to human chromosome 12p12-p13. Mol. Cell. Biol. *12*, 836–846.

Zhao, X., Lapalombella, R., Joshi, T., Cheney, C., Gowda, A., Hayden-Ledbetter, M.S., Baum, P.R., Lin, T.S., Jarjoura, D., Lehman, A., et al. (2007). Targeting CD37-positive lymphoid malignancies with a novel engineered small modular immunopharmaceutical. Blood *110*, 2569–2577.